Physica D 35 (1989) 357–381
North-Holland, Amsterdam

FINITE CORRELATION DIMENSION FOR STOCHASTIC SYSTEMS WITH POWER-LAW SPECTRA

A.R. OSBORNE and A. PROVENZALE
Istituto di Cosmo-Geofisica del C.N.R., Corso Fiume 4, Torino 10133, Italy

Received 29 July 1988
Revised manuscript received 11 November 1988
Accepted 26 November 1988
Communicated by H. Flaschka

We discuss a counter-example to the traditional view that stochastic processes lead to a non-convergence of the correlation dimension in computed or measured time series. Specifically we show that a simple class of "colored" random noises characterized by a power-law power spectrum have a finite and predictable value for the correlation dimension. These results have implications on the experimental study of deterministic chaos as they indicate that the sole observation of a finite fractal dimension from the analysis of a time series is not sufficient to infer the presence of a strange attractor in the system dynamics. We demonstrate that the types of random noises considered herein may be given an interpretation in terms of their fractal properties. The consequent exploitation of the non-Gaussian behavior of these random noises leads us to the introduction of a new time series analysis method which we call multivariate scaling analysis. We apply this approach to characterize several "global" properties of random noise.

1. Introduction

In recent years the phenomenological study of systems with irregular and unpredictable behavior have benefited from the development of a variety of new time series analysis techniques based on dynamical systems theory [2, 4, 9, 10, 14, 16, 17, 18, 32, 38, 39, 42, 43]. One of the most important physical cases studied with these methods occurs for forced, dissipative systems in which the low-dimensional chaotic dynamics is often associated with the presence of a strange attractor in the system phase space. The various methods provide estimates of properties of the attractor such as the fractal (Hausdorff) dimension, the spectrum of Lyapunov exponents and the Kolmogorov–Sinai entropy of the system. Experimental evidence of low-dimensional chaos has been obtained in several detailed analyses of carefully controlled laboratory systems (see for example [5, 7, 8, 19, 24, 38] for results in fluid dynamics). Owing largely to the ingenuity of many experimenters and to methods such as that proposed by Grassberger and Procaccia for computing the correlation dimension [16] and the correlation (K_2) entropy [17] of strange attractors, the study of deterministic chaos has undergone a transition from purely mathematical and theoretical results to the quantitative determination of chaotic effects in experimental data.

Among the various methods available for extracting phase space information from experimental data, the calculation of the fractal dimension has probably received the widest attention. The central idea behind the application of this approach is that systems whose dynamics are governed by stochastic processes are thought to have an infinite value for the fractal dimension. On the other hand a finite, non-integer value of the dimension is considered to be a strong indication of the presence of deterministic chaos. This is be-

cause random processes are thought to fill very large-dimensional subsets of the system phase space, while the existence of a low-dimensional chaotic attractor implies that only a rather low-dimensional subset of the phase space is asymptotically visited by the system motion.

From a physical point of view the most striking difference between a picture based on a stochastic description and the alternate approach based on deterministic chaos is essentially contained in the very different number of variables which are supposed, in the two cases, to characterize the system. If, given some irregular dynamics, one is able to show that the system is dominated by low-dimensional deterministic chaos, then an important physical result is that only a few (nonlinear and collective) modes are required to describe the system dynamics. This in turn implies that one could in principle substitute the original set of "primitive" partial differential equations with a small system of ordinary differential equations. For forced, dissipative systems in particular the number of variables needed to describe the dynamics has been shown to be strictly related to the attractor dimension (see Mané [27] and Takens [39]). If the system evolution is dominated by a strange attractor with fractal dimension D then an upper limit to the number of variables required to describe the dynamics may be fixed at $n = 2D + 1$. This in turn implies that *at most* $2D + 1$ ordinary differential equations are needed to rigorously describe the system evolution, if the appropriate collective variables can be defined. This is in sharp contrast to the behavior of systems dominated by a very large number of excited modes which are in general better described by stochastic or statistical models. Thus determining the presence of low-dimensional chaos from experimental data has important dynamical implications, and the calculation of the system fractal dimension is thought to be one of the steps toward this goal.

The physical implications discussed above, together with the relative simplicity of the methods for computing approximations to the fractal dimension, have recently stimulated a number of investigations on the behavior of *uncontrolled* natural or laboratory systems, and in several cases apparent evidence of low-dimensional chaos has been found [11, 12, 20, 21, 28, 35, 40]. In some cases however the supposed presence of a low-dimensional strange attractor was essentially based on the sole detection of a finite fractal dimension from the analysis of one or a few time series. The finite fractal dimension found from the data was then considered to be representative of the dimension of the underlying attractor.

An important comment about results of this type, however, is that although the relationship between the fractal dimension and the number of excited modes has a rigorous origin for systems which *are known* to be dominated by deterministic chaos, in an experimental context one in general does not know *a priori* if a low-dimensional attractor exists. But, apart from this problem, the observation of a finite fractal dimension from a measured signal has often been considered as *evidence* of low-dimensional chaos (and hence as a statement about the system dynamics). Thus a common conclusion has been that by a simple estimate of the system fractal dimension one can easily distinguish between random noise and low-dimensional chaos.

In the present paper we provide quantitative evidence that the traditional expectation of an infinite fractal dimension for a random signal may be misleading. *We discuss here a simple class of stochastic processes with power-law spectra which give a finite (and predictable) value for the fractal dimension*. This in turn implies that *the determination of a finite and non-integer value for the fractal dimension is in general not sufficient to indicate the presence of a strange attractor*. While this problem does not exist for the study of simple systems which are known to be dominated by low-dimensional deterministic dynamics, our results may have several important implications on the analysis of time series obtained from natural systems, results we discuss in detail below.

In the following quantitative analysis we use the method developed by Grassberger and Procaccia

[16] which has been proven to be a fast and reliable technique for computing the attractor dimension. The results are however completely independent of the particular method employed as they hold in general for all techniques for computing the fractal dimension. The ideas discussed here have been used in Osborne et al. [30] to interpret a set of Lagrangian observation of a large-scale turbulent flow in the Pacific Ocean; the data were characterized by a finite value of the correlation dimension, but we showed that this result was not due to the presence of a low-dimensional strange attractor.

The rest of this paper is organized as follows. In section 2 we briefly review the method of Grassberger and Procaccia for determining the fractal dimension. In section 3 we use this approach, together with Monte Carlo simulations of colored random noise, to demonstrate that systems of this type have a finite correlation dimension. An important issue which stems from these results is to determine whether the finite values of the correlation dimension found for this class of random signals have a physical or mathematical meaning. In section 4 we show how the values of the correlation dimension can be interpreted in terms of the fractal properties of the signals considered. A subsequent interpretation in terms of the non-Gaussian behavior of the joint probability densities of the amplitude scales of the signals is given in section 5. This last result leads to the introduction of a new method for the time series analysis of deterministic or stochastic dynamical systems which is based on a multivariate study of the amplitude scales of the system. In this latter approach "global" rather than local properties of the motion are emphasized. Conclusions are given in section 6.

2. The correlation dimension of strange attractors

In this section we briefly recall the method proposed by Grassberger and Procaccia [16] for computing the correlation dimension of strange attractors. Given a scalar time series $X(t_i)$ the first step is an embedding procedure to reconstruct a pseudo phase space for the system considered. A common way to obtain a reconstructed space is to use time embedding (see Packard et al. [32] and Takens [39]), in this case the vector time series is defined as

$$X(t_i) = \{ X(t_i), X(t_i+\tau), \ldots, X(t_i+(N-1)\tau) \}. \tag{2.1}$$

Here τ is an appropriate time delay multiple of the sampling time Δt and N is the dimension of the vector $X(t_i)$. The use of time embedding is not devoid of difficulty, however, as spurious correlations among the delayed variables can be generated if the time delay is badly chosen. See for example Atten et al. [1], Eckmann and Ruelle [9], and Fraser and Swinney [13] for a discussion of this problem. Different approaches to the reconstruction procedure have also been considered. One possibility is for example to take N independent measurements of the same dynamics, like the N time series generated by different initial conditions in the integration of numerical models (provided they belong to the same basin of attraction) or the time series measured by N close but spatially distinct Eulerian probes.

Given the vector time series $X(t_i)$, one defines the correlation function $C_N(\varepsilon)$ as

$$C_N(\varepsilon) = \frac{1}{M^2 - M} \sum_{i \neq j} H\{ \varepsilon - \| X(t_i) - X(t_j) \| \}, \tag{2.2}$$

where H is the Heaviside step function, M is the number of points in the vector time series $X(t_i)$ and the vertical bars indicate the norm of the vector. If an attractor for the system exists then

$$C_N(\varepsilon) \underset{\varepsilon \to 0}{\sim} \varepsilon^{\nu} \tag{2.3}$$

and

$$\nu_N \underset{N\to\infty}{\sim} \nu, \tag{2.4}$$

where ν is the correlation dimension of the attractor. For further details on this method see the original paper by Grassberger and Procaccia [16].

3. Finite correlation dimension for colored random noise

The method proposed by Grassberger and Procaccia has been developed for determining the dimension of the attractor, given that an attractor exists. As discussed above however, in the study of experimental data, this route has been somewhat reversed: If, given a measured time series from a dissipative system, an embedding procedure and the subsequent calculation of the correlation function leads to the determination of a finite value for ν through eqs. (2.3) and (2.4), then the system is often considered to be dominated by deterministic dynamics. If in addition the value of ν is small and non-integer then the system is thought to be dominated by low-dimensional chaos governed by the properties of a strange attractor. Systems dominated by stochastic processes are by contrast expected to provide a very different output. For random systems in fact the exponent ν_N is supposed not to saturate at any finite value ν but it is thought to increase without bound. The widely adopted example of white noise supports this view. In this section however we discuss a simple class of random noises with power-law spectra and we show how they provide a finite and well-defined value for the correlation dimension.

To quantitatively exploit this observation we consider the standard spectral expansion of a real random function (see e.g. Panchev [33])

$$X(t) = \int_0^\infty \cos \omega t \, \mathrm{d}Z_1(\omega) + \int_0^\infty \sin \omega t \, \mathrm{d}Z_2(\omega) \tag{3.1}$$

in the form of a Fourier-Stieltjes stochastic integral where $Z_1(\omega)$ and $Z_2(\omega)$ are real random functions with the properties (Yaglom [41])

$$\langle Z_1(\omega)\rangle = \langle Z_2(\omega)\rangle = 0, \tag{3.2a}$$

$$\langle [Z_i(\omega_1 + \Delta\omega_1) - Z_i(\omega_1)] \times [Z_i(\omega_2 + \Delta\omega_2) - Z_i(\omega_2)]\rangle = 0, \quad i = 1,2, \tag{3.2b}$$

$$\langle [Z_1(\omega + \Delta\omega) - Z_1(\omega)]^2\rangle = \langle [Z_2(\omega + \Delta\omega) - Z_2(\omega)]^2\rangle . \tag{3.2c}$$

The spectral expansion (3.1) is a well-known approach to the study of random functions. Further details and proofs about this approach may be found for example in Yaglom [41]. In numerical studies of random noise the spectrum of the random process is packed into a discrete series of frequencies $\omega_k = k\,\Delta\omega$, $k = 1, M/2$ and the random function is then computed as a discrete series at times $t_i = i\,\Delta t$, $i = 1, M$. In this case formula (3.1) reduces to a simple superposition of harmonic oscillations, i.e. to the standard Fourier series

$$X(t_i) = \sum_{k=1}^{M/2} a_k \cos(\omega_k t_i) + \sum_{k=1}^{M/2} b_k \sin(\omega_k t_i), \quad i = 1, M, \tag{3.3}$$

or equivalently

$$X(t_i) = \sum_{k=1}^{M/2} \zeta_k \cos(\omega_k t_i + \phi_k), \quad i = 1, M, \tag{3.4}$$

where $a_k = \zeta_k \cos(\phi_k)$ and $b_k = -\zeta_k \sin(\phi_k)$. The coefficients ζ_k are related to the power spectrum $P(\omega_k)$ of the random function by

$$\zeta_k = [P(\omega_k)\,\Delta\omega]^{1/2} \tag{3.5}$$

and the ϕ_k's are the (random) phases. Standard results on the discrete Fourier series require that $\Delta\omega = 2\pi/T$ where $T = M\Delta t$ is the length of the time series and that the spectrum has a high-frequency cutoff at the Nyquist frequency $\omega_{max} = (M/2)\Delta\omega = \pi/\Delta t$; for further details on these results see for example Panchev [33] and Rice [36]. One approach to the problem of generating a random signal is to select the set of the $\{a_k\}$ and the $\{b_k\}$ as Gaussianly distributed random variables. Another simple and widely adopted method is to consider a fixed power spectrum and uniformly distributed random phases (see for example Rice [36], Osborne [29]).

In this study we are interested in signals of the form (3.4) whose power spectrum has a power-law dependence

$$P(\omega_k) = C\omega_k^{-\alpha} \tag{3.6}$$

and the phases are randomly, uniformly distributed on the interval $(0, 2\pi)$. The choice of a power-law spectrum is physically significant since many experimental measurements from widely different systems have approximate power-law spectra. For example 3-D turbulence, 2-D and geostrophic turbulence [23, 31, 33, 37], internal waves in the ocean [15], passively advected scalars [3] and drifter trajectories in large-scale flows [30] are well-known examples in fluid flows. In what follows each time series obtained by inverting the spectrum (3.6) for a fixed value of α (i.e. obtained using eq. (3.4)) is a particular realization of a member of this one parameter (α) family of "colored" random noises. Each choice of the set of random phases corresponds to a different realization of the same stochastic process. The constant C in the spectrum is fixed by the requirement that the time series have unit variance.

To proceed with the analysis we have selected a number of values of the spectral exponent α and for each of these we have generated fifteen independent realizations of the process, say $x_n(t_i; \alpha)$, where $i = 1, M$ and $n = 1, 15$. The latter notation in x_n indicates that each process is viewed as a function of the spectral exponent α. In what follows the upper case notation X is used for generic time series while the lower case x is reserved for time series obtained by formulas (3.4) and (3.6). The number of points in each realization $x_n(t_i; \alpha)$ is $M = 8192$ and each time series corresponds to a different choice of the set of random phases. The goal is to search for convergence in the calculated value of the correlation dimension and, in the case of convergence, to see whether a relation may be found between the spectral exponent and the value of the correlation dimension.

To this end we use the following embedding procedure: For each selected value of the spectral exponent α we consider fifteen different embedding spaces with dimension N, where we used $1 \le N \le 15$. An N-dimensional curve $x(t_i; \alpha)$ is obtained by taking N independent realizations $x_n(t_i; \alpha)$, $n = 1, N$ of the random process for the selected value of α. The alternative use of a time embedding procedure with N time delayed values of a single realization of the random process is substantially similar and, under appropriate conditions, leads to the same results. This is briefly discussed in the appendix. Here we use independent realizations to insure that the results are not an artifact of the spurious correlations possibly introduced by time embedding.

We first computed time series of 8192 points for the N-dimensional state vector $x(t_i; \alpha)$. We then computed the correlation functions $C_N(\varepsilon)$ for $N = 1, 2, \ldots, 15$ and searched for scaling behavior in each of the functions $C_N(\varepsilon)$. If scaling holds for every N then one can define the exponents ν_N through eq. (2.3) and study their behavior for increasing N. The usual expectation would be that the ν_N's do not saturate at a finite value for increasing N in the case of a random process.

In fig. 1(a) we show the fifteen correlation functions $C_N(\varepsilon)$ for $N = 1, \ldots, 15$ when a value $\alpha = 1.0$ of the spectral exponent is chosen. This corresponds to a white noise spectrum. A scaling region is evident (each $C_N(\varepsilon)$ is a straight line on the log–log plot) and consequently the values of the

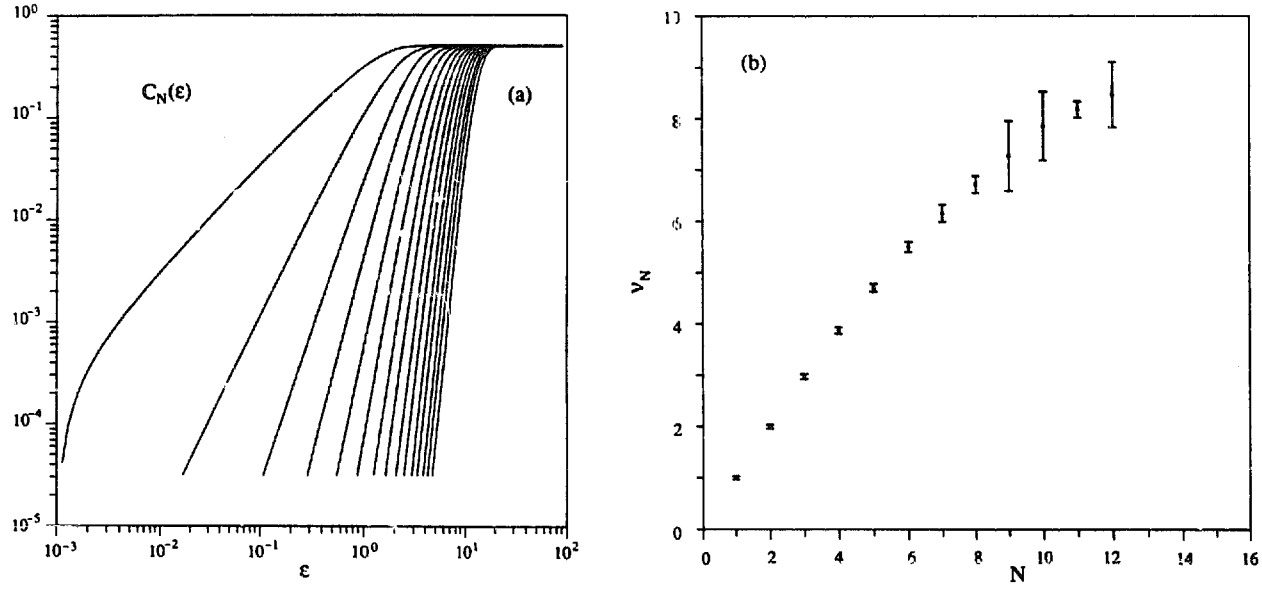

Fig. 1. (a) The fifteen correlation functions $C_N(\varepsilon)$ for a spectral exponent $\alpha = 1.0$, and (b) the correlation dimension ν_N versus the embedding dimension N for this case. No saturation is evident in this case.

various ν_N can be determined. Fig. 1(b) shows ν_N versus N, no evident saturation is present as traditionally expected. The error bars on the individual values of ν_N are purely statistical and represent the 95% confidence limits of the least-squares fit of $\log C_N(\varepsilon)$ versus $\log \varepsilon$.

Fig. 2(a) shows $C_N(\varepsilon)$, $N = 1,\ldots,15$ for the case $\alpha = 1.75$. Again scaling is evident, but the situation is now quite different from that found for $\alpha = 1.0$. The values of ν_N can be easily defined for each N, and as shown in fig. 2(b) they *do* saturate at a finite value $\nu \cong 2.66$ when n is increased. This traditionally unexpected result thus implies that a finite value for the correlation dimension ν may be found even for non-deterministic, random signals.

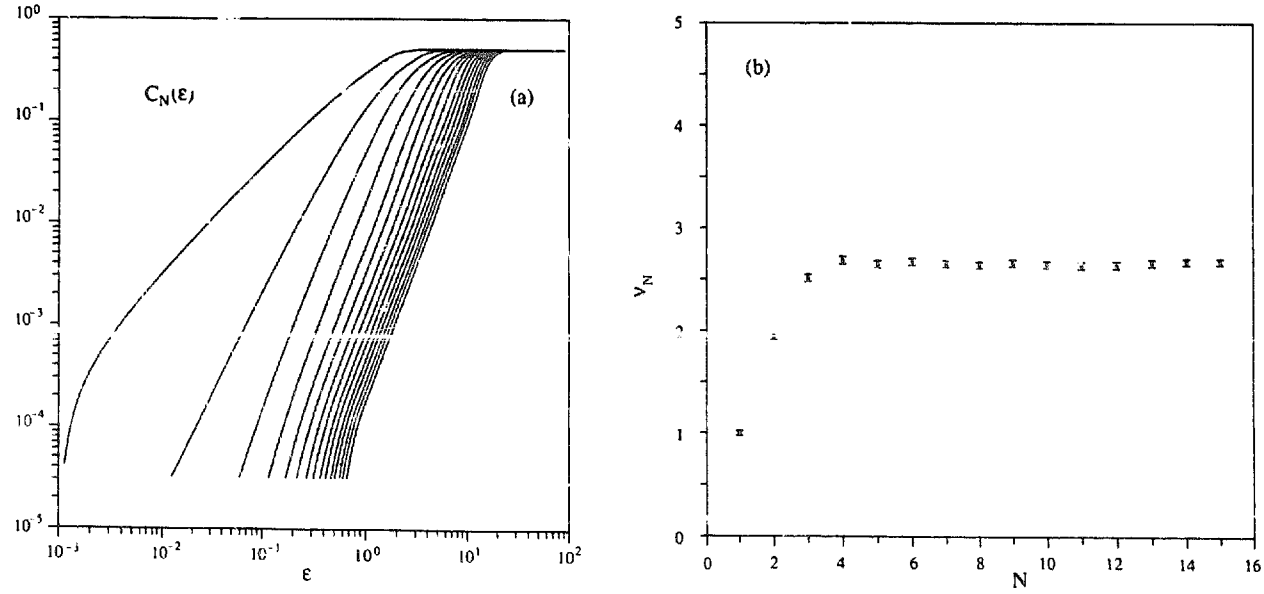

Fig. 2. (a) The fifteen correlation functions $C_N(\varepsilon)$ for $\alpha = 1.75$, and (b) the dimension ν_N versus N. The correlation dimension saturates at a value $\nu \cong 2.66$.

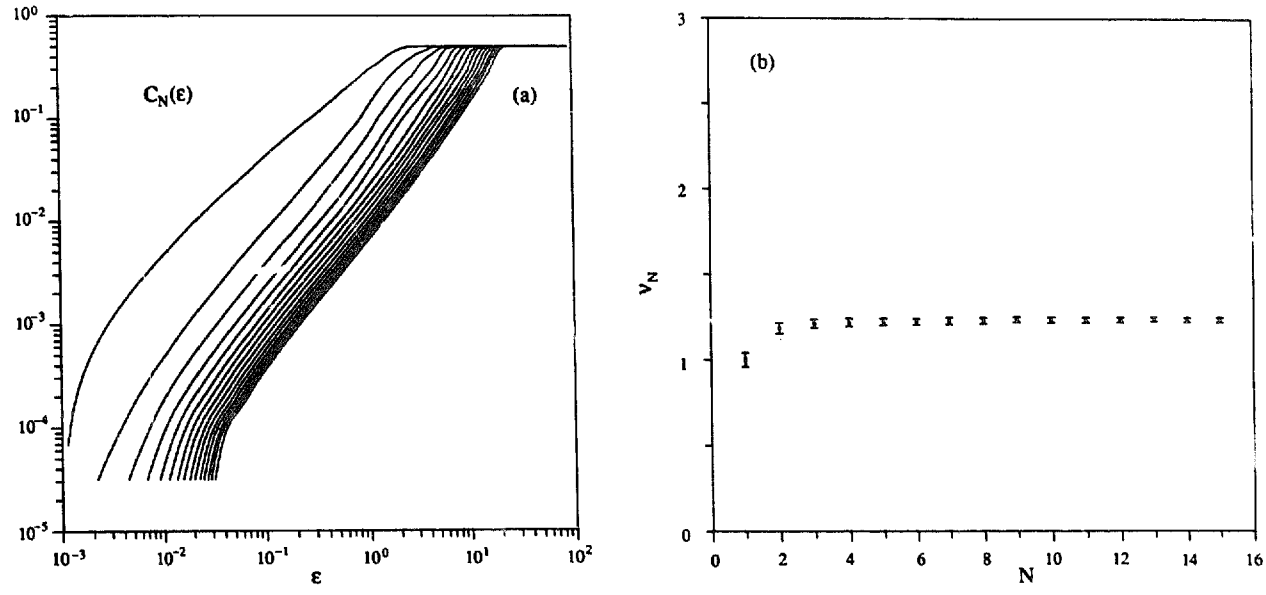

Fig. 3. (a) The fifteen correlation functions $C_N(\varepsilon)$ for $\alpha = 2.75$, and (b) the dimension ν_N versus N. The correlation dimension saturates at a value $\nu \cong 1.22$.

In fig. 3 we show a further example of this behavior for a spectral exponent $\alpha = 2.75$. Again there is an evident scaling range in the correlation functions, and the plot of ν_N versus N reported in fig. 3(b) show the saturation of ν_N to the small value $\nu \cong 1.23$ for the correlation dimension.

From the above figures one can see that the scaling region is limited at very small values of $C_N(\varepsilon)$ by a "knee" in the correlation function. This behavior is well known in the analysis of computer generated or experimental data (see for example Eckmann and Ruelle [9]) and is due either to the presence of experimental or numerical errors or, more importantly, to the lack of statistics at small scales induced by the finite length of the signals analyzed. This however presents no difficulty in the analysis as long as the scaling region is sufficiently large.

Repeating the above analysis for a number of values of the spectral exponent α allows one to search for a quantitative relation between the exponent α and the correlation dimension ν. Table I reports the results for several values of the spectral exponent and fig. 4 shows the correlation dimension versus the exponent α. For each value of α the dimension ν has been determined as the average of the individual values ν_N for $N > N_0$, where N_0 is the phase space dimension beyond which no systematic increase of ν_N is observed. The error bars in table I and in fig. 4 represent the standard deviation of the average dimension for $N > N_0$. It is evident how the correlation dimension is a well-defined monotonically decreasing function $\nu(\alpha)$ of the spectral exponent α for this class of

Table I

Spectral exponent α	Correlation dimension ν
1.00	> 10
1.25	6.110 ± 0.090
1.50	3.749 ± 0.015
1.75	2.656 ± 0.013
2.00	2.053 ± 0.009
2.25	1.661 ± 0.007
2.50	1.403 ± 0.006
2.75	1.234 ± 0.005
3.00	1.140 ± 0.005
3.25	1.084 ± 0.004
3.50	1.058 ± 0.004
3.75	1.046 ± 0.004
4.00	1.041 ± 0.005
4.25	1.038 ± 0.004
4.50	1.038 ± 0.005
4.75	1.037 ± 0.004
5.00	1.025 ± 0.004

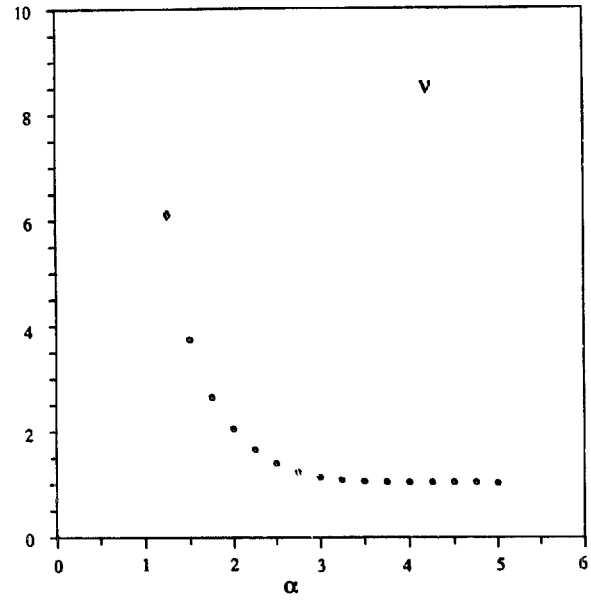

Fig. 4. The correlation dimension ν versus the spectral exponent α. The correlation dimension is a well-defined, monotonically decreasing function $\nu(\alpha)$ of the spectral exponent α for this class of random noises.

Table II

Realization number	Correlation dimension ν
1	2.053 ± 0.004
2	2.077 ± 0.016
3	2.061 ± 0.010
4	2.050 ± 0.010
5	2.049 ± 0.009
6	2.088 ± 0.011
7	2.041 ± 0.013
8	2.045 ± 0.009
9	2.057 ± 0.009
10	2.077 ± 0.010
11	2.095 ± 0.010
12	2.043 ± 0.009
13	2.052 ± 0.011
14	2.062 ± 0.012
15	2.055 ± 0.009
16	2.081 ± 0.029
17	2.075 ± 0.012
18	2.072 ± 0.009
19	2.047 ± 0.010
20	2.054 ± 0.008

random processes. From fig. 4 one realizes that the expectation of a non-saturating dimension is really satisfied in the case of white noise, but it is *not* true in general for random noises with power-law spectra.

Before discussing the interpretation of these results we now briefly explore the effects of a) changing the set of random phases (i.e. considering several different realizations of the same random process); and b) changing the length T of the time series and the time step Δt.

To study the effect of changing the set of random phases we have considered twenty ensembles of 15-dimensional curves (each curve being composed of fifteen realizations of the same random process), and we have computed the correlation dimension for each member of the ensemble. As an example table II reports the twenty values of ν obtained in the case $\alpha = 2$ (with $M = 8192$) and fig. 5 shows the distribution of the values of ν. The values of the correlation dimension obtained from the various members of the ensemble are closely grouped around the mean value $\langle \nu \rangle = 2.062$, the standard deviation of the average being $\sigma_{\langle \nu \rangle} = 0.004$. The same behavior is observed in general for all the values of α considered in this study. Thus we conclude that the dependence of the correlation dimension on the spectral exponent α is not affected by the particular set of random phases chosen in eq. (3.4) (apart from numerical and statistical fluctuations, which are in any event quite small).

Of greater interest is perhaps the dependence of $\nu(\alpha)$ on the length of the time series and on the time step Δt. To explore this problem we have repeated the calculation of the correlation dimension for several values of α and M varying from 64 to 16,384 with fixed Δt. This is a test on the effects of changing the length T of the time series and corresponds to decreasing $\Delta\omega = 2\pi/T$ in the spectrum. We have found that: a) The "knee" in the graphical representation of the correlation functions is found at larger scales for smaller values of M. This is related to the increased lack of statistics at small scales for short time series. b) Decreasing the number of points in the time series

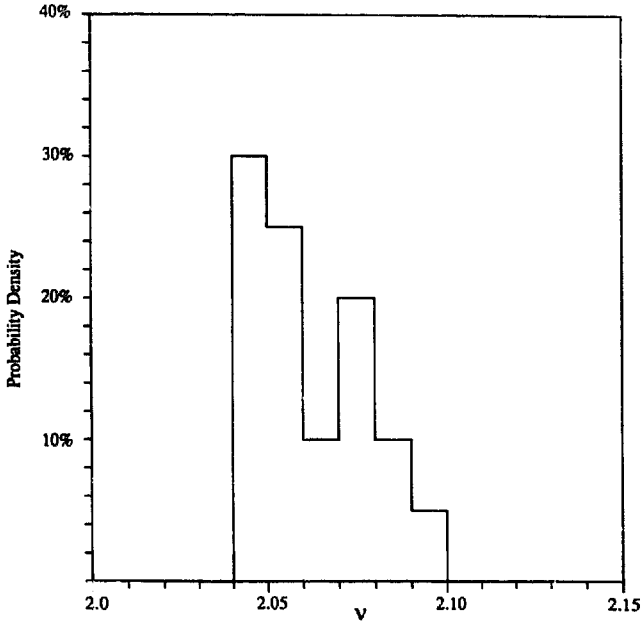

Fig. 5. Histogram of the values of the correlation dimension found in the case $\alpha = 2$ for twenty different realizations of the fifteen-dimensional curve $x(t_i; \alpha)$.

results in larger fluctuations of the correlation dimension from one realization to another. With a limited number of points (e.g. $M \approx 500$) one may observe fluctuations in the value of the correlation dimension of the order of 15%. c) The average value of the correlation dimension increases for decreasing M (with Δt fixed). For example for $\alpha = 2.75$ we observed $\nu \cong 1.15$ with 8192 points and $\nu \cong 1.5$ with 64 points. In general however, for a reasonable number of points (say larger than approximately 500) the estimates of the correlation dimension are quite stable and do not differ much from the estimates obtained with longer time series.

Alternativley we have fixed the value of $T = M\Delta t$ and we have decreased Δt (increasing M correspondingly). This is equivalent to increasing the Nyquist cutoff $\omega_{max} = \pi/\Delta t$ in the spectrum of the signal. The results again indicate the stability of the estimates of the correlation dimension and the convergence to a well-defined value for decreasing Δt. Consequently the finite dimensions determined for the random signals considered here are not an artifact of short time series or of an inappropriate choice of Δt. In the next section we discuss how these finite values of the correlation dimension can be theoretically predicted (in agreement with the numerical results discussed here) and we elucidate their origin.

4. An interpretation in terms of fractal curves

In the previous section we have shown how a well-defined curve $\nu(\alpha)$ apparently determines the value of the correlation dimension as a function of the spectral exponent for the class of random noises considered herein. This relation is very stable and is not affected by the choice of the set of random phases or by the kind of embedding adopted (see appendix). Now the obvious question arises as to whether these values of the correlation dimension have any physical or mathematical meaning. It is clear that they are not related to any deterministic dynamical process. Here we discuss how these values of ν are related to the fractal properties of the time series generated by inverting power-law spectra with the Fourier series (3.4).

A brief definition of a fractal set is "a mathematical object whose topological dimension is strictly smaller than its Hausdorff dimension" [25, 26]. In dynamical systems theory a strange attractor (of a system of differential equations) with fractal dimension $D > 1$ is an object which is differentiable along the direction of motion and which can be "fractal" in some direction perpendicular to the direction of motion. Fractal curves however exist which are everywhere continuous and non-differentiable. Examples are the various types of fractal "random paths" such as classic Brownian motion. These paths are realizations of a stochastic process and they possess a finite Hausdorff dimension which may be larger than their topological dimension.

A particularly important and simple class of fractal random paths are self-similar fractal curves. This property can hold both in a deterministic sense, i.e. a curve built by a deterministic algo-

rithm, or in a statistical sense. In the latter case self-similarity refers to the probability distributions of the random process which generates the curve.

To properly understand self-similar fractal curves it is appropriate to introduce self-affine signals. To this end consider an arbitrary random scalar function of time, say $X(t_i)$ (we have supposed here a discrete time, having in mind the application of these ideas to experimental or numerical time series). If

$$\lambda^{-H}[X(t_i+\lambda\,\Delta t)-X(t_i)] \overset{d}{=} [X(t_i+\Delta t)-X(t_i)] \tag{4.1}$$

holds independent of time ($\overset{d}{=}$ means equality in the sense of distributions) then $X(t_i)$ is said to be self-affine with scaling exponent H. This exponent must be positive and less than or equal to one. From a practical point of view self-affinity means that if the time scale is rescaled by a factor λ and the signal itself is rescaled by a factor λ^{-H} then the transformed time series has the same statistical properties as the original one.

To pass from self-affine signals to self-similar paths in an N-dimensional space one can consider N independent realizations of the given random process, say $X_n(t_i)$, $n=1, N$. The N time series $X_n(t_i)$ are different realizations of the same random process and they all have the same scaling exponent H. These N time series can thus be thought of as the parametric equations of a curve which is a "random path" in an N-dimensional space. It can be shown that this trajectory is self-similar in the statistical sense: If we rescale by the same factor the scales of the N axes of the space, then the rescaled trajectory has the same statistical properties as the original one. The fractal dimension of the trajectory is then given by (see for example Mandelbrot [25, 26])

$$D=\min\{1/H, N\}. \tag{4.2}$$

Thus for $0<H<1$ the trajectory is a fractal curve, as its fractal dimension is strictly larger than its topological dimension, $D_T=1$. Studying the scaling properties of the individual components, i.e. of the scalar random functions $X_n(t_i)$, of a self-similar fractal curve is thus a typical way of obtaining its fractal dimension.

From formula (4.2) one sees that the fractal dimension of a curve in a space cannot exceed the topological dimension of the space. If a fractal curve with Hausdorff dimension D is embedded in an N-dimensional space then the curve completely "fills" the embedding space as long as $N<D$, but it only fills a lower-dimensional subset of the space if $N>D$. Computing the fractal (or correlation, etc.) dimension of the curve by varying the embedding dimension N thus provides a fractal dimension which increases with N until the space dimensionality exceeds the fractal dimension of the curve. At this point the calculated fractal dimension does not change further for increasing N, i.e. it saturates at the correct value D.

The interpretation of the finite correlation dimensions found for the random processes studied in the previous section is now clear. The curves generated by inverting power-law spectra and random phases are random fractal paths. Their Hausdorff dimension is finite, and thus their correlation dimension is finite as well. The Grassberger and Procaccia approach is independent of the ordering of the points in the signal and is not able to test the differentiability of the curve under study. Thus this method cannot distinguish between fractal attractors and fractal random curves if the two have the same dimension.

To quantitively assess the interpretation of colored random noises in terms of fractals we now use two typical properties of random fractal curves. First we compute the scaling exponent H from each time series obtained by inverting power-law spectra and random phases. This allows the calculation of the Hausdorff dimension through eq. (4.2). To search for statistical self-affinity and to compute the scaling exponent H from a random time series we concentrate on the average absolute

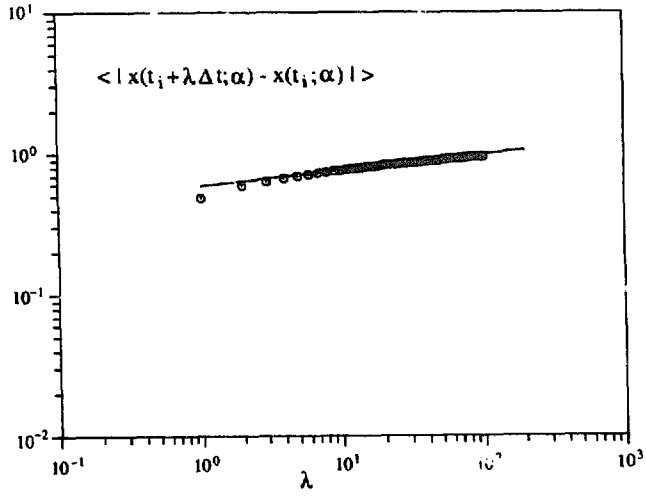

Fig. 6. Average absolute values of "jumps" (as defined in the text) versus λ in log–log coordinates for the case $\alpha = 1.0$. The slope of the least-squares-fit line to the numerical data provides the value of the scaling exponent H.

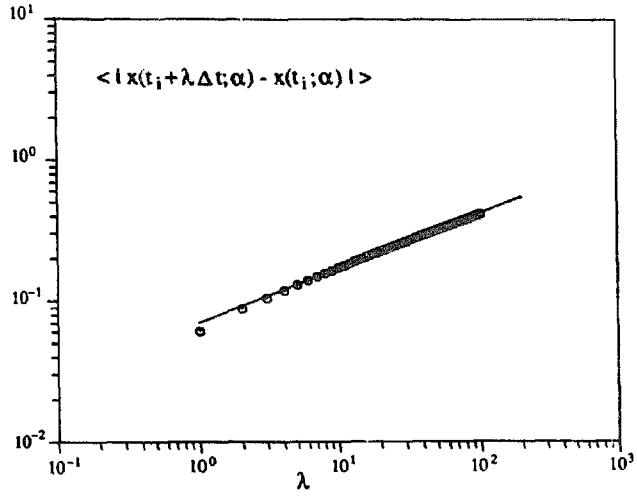

Fig. 7. Average absolute values of "jumps" versus λ for the case $\alpha = 1.75$.

value of a "jump", i.e. if the signal is self-affine then

$$\left\langle |x(t_i + \lambda\,\Delta t;\alpha) - x(t_i;\alpha)| \right\rangle = \lambda^H \left\langle |x(t_i + \Delta t;\alpha) - x(t_i;\alpha)| \right\rangle, \qquad (4.3)$$

where $\lambda\,\Delta t$ is an integer multiple of the sampling time Δt, the vertical bars denote the absolute value and $\langle\ \rangle$ indicates average over all points in the time series (i.e. a time average) and over all the fifteen realizations of the random process for a fixed value of α. If the signal is self-affine a graph of $\langle |x(t_i + \lambda\,\Delta t;\alpha) - x(t_i;\alpha)| \rangle$ versus λ on a log–log plot is a straight line whose slope is the value of H. Fig. 6 shows $\langle |x(t_i + \lambda\,\Delta t;\alpha) - x(t_i;\alpha)| \rangle$ versus λ for $\alpha = 1.0$. A small slope is seen which gives $H \cong 0.1$, thus furnishing $D = 1/H \cong 10$. In fig. 7 we report the case for $\alpha = 1.75$, obtaining $H \cong 0.39$ and thus $D \cong 2.56$. In fig. 8 the case for $\alpha = 2.75$ is shown. The slope of the curve is $H \cong 0.84$ giving $D \cong 1.19$. We have repeated this analysis for all the values of α already considered in the calculation of the correlation dimension. In table III we report the values of H and of $D = 1/H$ and in fig. 9 we report the values of $D = 1/H$ versus α. The error bars are the 95% confidence limits of the least-squares fits. The two curves shown in fig. 9 are theoretical curves which are discussed at the end of this section. The results of the calculation of the scaling exponent H and consequently of $D = 1/H$ provide evidence that the random paths with power-law spectra studied here are self-similar fractal curves.

Our second analysis on the fractal nature of these random processes is based on obtaining the dimension of the curves by measuring their length by different rulers. If the length is approximated by a broken line whose segments have a "yard-

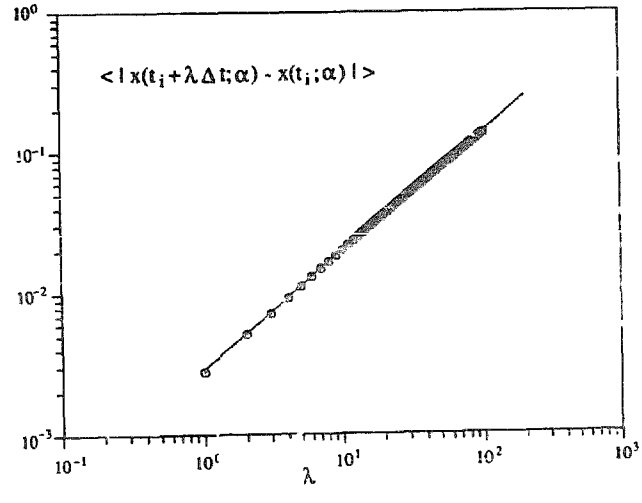

Fig. 8. Average absolute values of "jumps" versus λ for the case $\alpha = 2.75$.

Table III

Spectral exponent α	Scaling exponent H	Scaling dimension $D = 1/H$
1.00	0.109 ± 0.003	9.174 ± 0.253
1.25	0.185 ± 0.003	5.405 ± 0.088
1.50	0.280 ± 0.002	3.571 ± 0.026
1.75	0.389 ± 0.002	2.571 ± 0.013
2.00	0.505 ± 0.001	1.980 ± 0.004
2.25	0.624 ± 0.001	1.603 ± 0.003
2.50	0.738 ± 0.001	1.355 ± 0.002
2.75	0.839 ± 0.001	1.192 ± 0.002
3.00	0.914 ± 0.002	1.094 ± 0.002
3.25	0.961 ± 0.001	1.041 ± 0.001
3.50	0.985 ± 0.001	1.015 ± 0.001
3.75	0.995 ± 0.001	1.005 ± 0.001
4.00	0.999 ± 0.001	1.001 ± 0.001
4.25	1.000 ± 0.001	1.000 ± 0.001
4.50	1.000 ± 0.001	1.000 ± 0.001
4.75	1.000 ± 0.001	1.000 ± 0.001
5.00	1.000 ± 0.001	1.000 ± 0.001

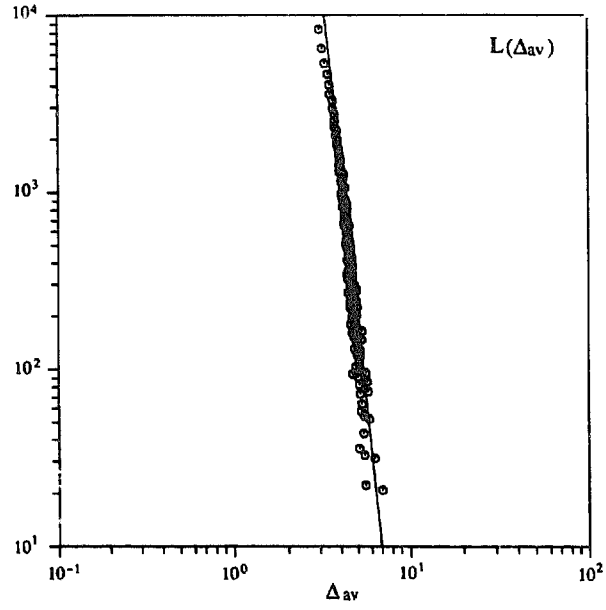

Fig. 10. Length of the curve $x(t_i)$ in the fifteen-dimensional space versus the yardstick length Δ for the case $\alpha = 1.0$. The strong divergence of the length indicates the fractal nature of this curve and reflects its large dimensionality.

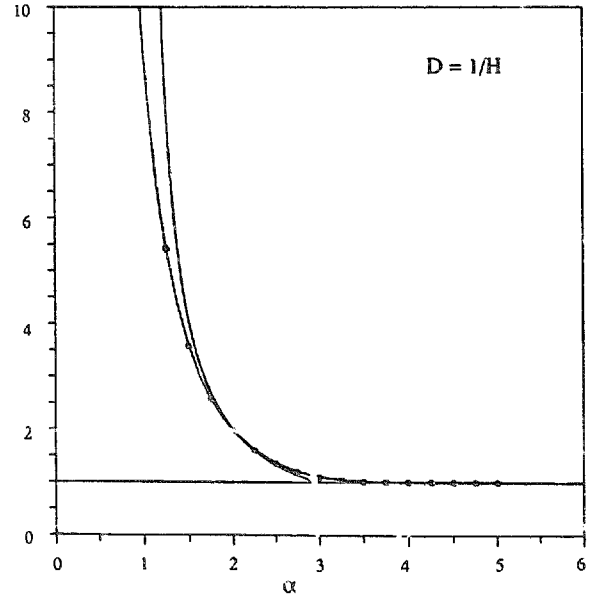

Fig. 9. The fractal dimension D, determined as the inverse of the scaling exponent, versus the spectral exponent α. These results indicate the fractal and self-affine nature of the random noises studied here. The values of the fractal dimension $D = 1/H$ are in excellent agreement with the values of the correlation dimension shown in fig. 4. The solid and the dashed lines are theoretical relationships for respectively "perfect" and truncated power-law spectra and are discussed in the text.

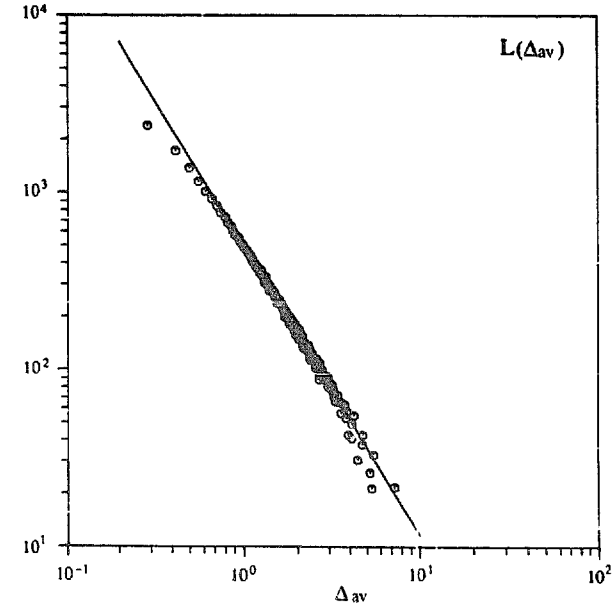

Fig. 11. Length of the curve $x(t_i)$ versus Δ for $\alpha = 1.75$. Again a divergence is observed which implies a fractal character of the curve. The divider dimension is $D_L \cong 2.64$.

stick" length Δ then in the limit for small Δ the curve length $L(\Delta)$ goes as

$$L(\Delta) = \Delta^{1-D_L}, \tag{4.4}$$

where D_L is the "divider dimension" and approximates the Hausdorff dimension D [25, 26]. For an analytic curve $D_L = 1$ and one obtains the ordinary length of a differentiable curve. For fractal curves the length diverges for smaller and smaller yardstick lengths. Computing the power law in (4.4) of the length divergence of a fractal curve furnishes its fractal dimension.

Because the points in the random curves considered here are equally spaced in time but not in space, we cannot however consider a fixed yardstick length Δ in applying the above method. The simplest solution to this problem is to compute the curve length $L(\Delta_{av})$ versus the average length Δ_{av} of the yardstick. We find that this procedure furnishes the divider dimension D_L with negligible error. Fig. 10 shows $L(\Delta_{av})$ versus Δ_{av} for $\alpha = 1.0$. A strong divergence with power-law dependence from Δ_{av} is observed, which corresponds to a dimension $D_L \cong 10$. The case for $\alpha = 1.75$ is shown in fig. 11, divergence is again observed (indicating the fractal, non-differentiable character of the curve) with $D_L = 2.64$. In fig. 12 the case for $\alpha = 2.75$ is shown, here a slight divergence is evident which gives $D_L = 1.22$. Again the analysis has been repeated for many values of α. In table IV we report the values of D_L obtained and in fig. 13 we show the values of D_L versus α. The error bars are the 95% confidence limits of the least-squares fit of $\log L(\Delta_{av})$ versus Δ_{av}.

From the above analysis it is clear that excellent agreement is generally observed among the values of the fractal dimension determined by the correlation function approach, by the yardstick length method and by the scaling exponent calculations. These results confirm that a) the random paths generated by inverting power-law spectra and random Fourier phases are random fractal curves whose dimension is determined by the spectral exponent and b) these random paths have finite

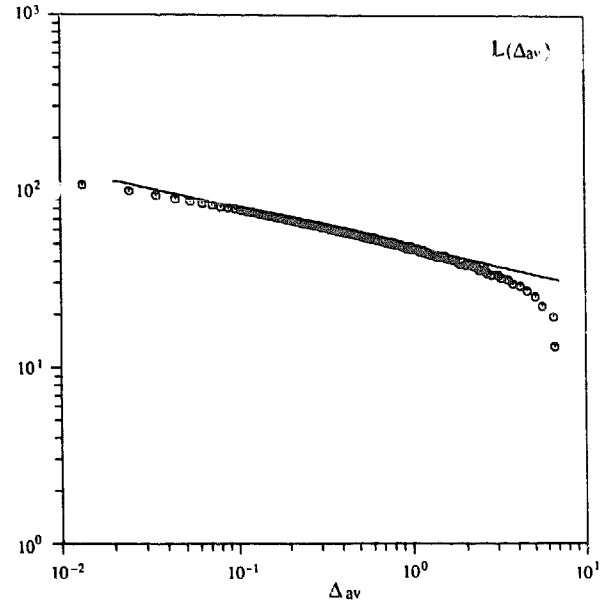

Fig. 12. Length of the curve $x(t_i)$ versus Δ for $\alpha = 2.75$. The divergence indicates a value of the divider dimension $D_L \cong 1.22$.

correlation dimension as well, whose value in this case does not measure the dynamical properties of the system under study but only the fractal nature of the curves. This point is worth discussing further. The common methods for computing the fractal dimension (or an approximation such as

Table IV

Spectral exponent α	Divider dimension D_L
1.00	10.265 ± 0.862
1.25	6.044 ± 0.196
1.50	3.792 ± 0.070
1.75	2.639 ± 0.020
2.00	2.021 ± 0.010
2.25	1.632 ± 0.005
2.50	1.376 ± 0.001
2.75	1.222 ± 0.003
3.00	1.127 ± 0.002
3.25	1.046 ± 0.001
3.50	1.022 ± 0.001
3.75	1.011 ± 0.001
4.00	1.006 ± 0.001
4.25	1.004 ± 0.001
4.50	1.003 ± 0.001
4.75	1.002 ± 0.001
5.00	1.002 ± 0.001

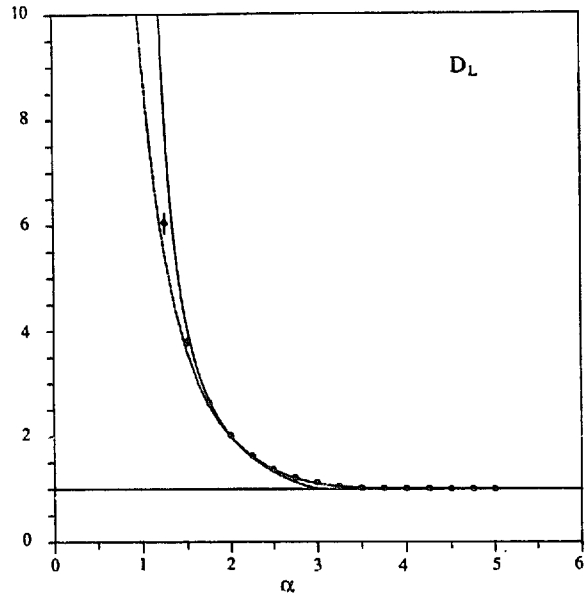

Fig. 13. Divider dimension D_L versus the spectral exponent α. These values of the dimension agree with both the dimensions obtained from the scaling exponent and the values of the correlation dimension. The solid and the dashed lines are theoretical relationships for respectively "perfect" and truncated power-law spectra and are discussed in the text.

the correlation dimension) do not test the dynamics of the system, since they are purely statistical procedures which are independent of the ordering of the points in the time series. All these methods focus on small space scale properties of the system (limit for $\varepsilon \to 0$). If the fractality is generated by deterministic chaotic dynamics then small space scales are associated with long time scales (close returns on the attractor). If on the other hand the system is a stochastic fractal then the small space scales are related to small time scales. But procedures such as the Grassberger and Procaccia method cannot distinguish between the two possibilities.

As already mentioned above, in figs. 9 and 13 two theoretical curves are drawn together with the results of the numerical analysis. There is in fact a close theoretical relationship between self-affine signals and their power spectra. Self-affinity implies that there is no preferred length scale in the dynamics. A well-known classic argument, which relates the structure function of a signal with a power-law spectrum to the spectral exponent, indicates that a self-affine signal has a power-law spectrum $P(\omega) = C\omega^{-\alpha}$ with $\alpha = 2H + 1$ (see Panchev [33]). The fractal dimension of a curve is thus related to the slope of the power spectrum of each of its components (if they are independent and have the same scaling exponent H) by the equation

$$D = 2/(\alpha - 1). \tag{4.5}$$

The constraint $0 < H < 1$ and the requirements on the convergence of the integral which defines the structure function make eq. (4.5) valid only for $1 < \alpha < 3$. For $\alpha > 3$ the Hausdorff dimension of the curve is equal to its topological dimension and the curve ceases to be fractal. For $0 \le \alpha \le 1$ the scaling exponent is zero and the fractal dimension has an unbounded (infinite) value, i.e. the signal in this case actually generates a non-saturating fractal dimension. Eq. (4.5) has been used to generate the solid curve shown in figs. 9 and 13.

From the above figures one realizes that there is a good overall agreement between the theoretical curve given by eq. (4.5) and the dimension estimates obtained by the numerical analysis. Significant differences occur however for $\alpha \approx 1$ and $\alpha \approx 3$. The numerical results are systematically below the theoretical curve for $\alpha \approx 1$ and above it for $\alpha \approx 3$. Careful study of these effects led us to the conclusion that these discrepancies may be entirely understood in terms of the low- and high-frequency cutoffs to the power spectrum implied by the use of numerical (or experimental) data. The low-frequency cutoff $\Delta\omega$ in the spectrum corresponds to the finite length T of the time series, $\Delta\omega = 2\pi/T$. The high-frequency (Nyquist) cutoff ω_{max} is in turn associated with the finiteness of the sampling interval Δt, $\omega_{max} = \pi/\Delta t$. When the total length T is increased and the sampling time Δt is decreased the deviations tend (although very slowly) to disappear and the numerical values of the fractal dimension become closer to the theoretical curve. A generalized theoretical expression for $\nu(\alpha)$ may be exactly obtained for finite values of T and Δt. This expression corresponds to a spectral

expansion of the random process such as formula (3.1) with both finite lower and upper limits in the integral. The dashed curves in figs. 9 and 13 represent this generalized theoretical relation for $\Delta t = 1$ and $T = 8192$. Excellent agreement is found between the numerical estimates of the dimension and this generalized theoretical relationship. Further details on these issues will be discussed in a forthcoming paper.

5. Multivariate scaling analysis and non-Gaussian behaviour

In the previous section the finite values of the correlation dimension have been shown to be generated by the fractal nature of the random processes. These fractal properties and the power-law dependence of the power spectra are however also related to non-Gaussian statistical behavior. This is understood in terms of a failure of the central limit theorem since the power-law form of the spectrum determines an infinite (theoretical) variance for the low-frequency components. Thus one of the assumptions necessary for convergence to a Gaussian distribution is violated. For spectra with a low-frequency cutoff (such as the spectra encountered in numerical or experimental studies) the variance of the low-frequency components is not infinite but is still much larger than the variance of the other Fourier components, and thus (for practical purposes) non-Gaussian distributions have to be expected also in this case.

The non-Gaussian nature of the processes is illustrated in fig. 14 where we show the amplitude probability densities for random noises with power-law spectra and random phases for $\alpha = 1.00$, $\alpha = 1.75$ and $\alpha = 2.75$. As expected from the discussion above the deviations from a Gaussian distribution become more pronounced with increasing α. This is because for larger α, there is a large relative weight of the low-frequency components in the spectrum.

The non-Gaussian statistical properties of this class of random noises have also a direct relation-

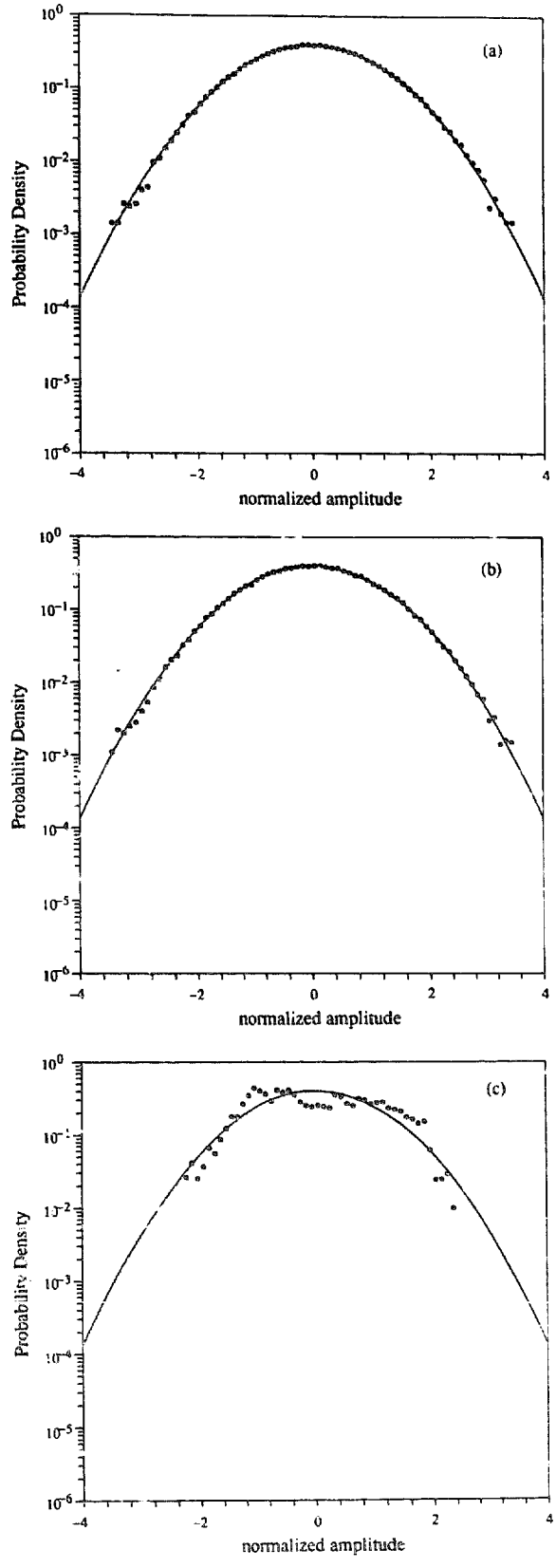

Fig. 14. Probability densities of the signal amplitudes for the cases (a) $\alpha = 1.0$, (b) $\alpha = 1.75$, (c) $\alpha = 2.75$. The larger is α, the more pronounced are the deviations from Gaussian behavior.

ship to their fractal dimension and they can be fruitfully studied in what we can define as *the scaling space* of the system. Determination of the system statistical properties in this space provides a new time series analysis method which we call *multivariate scaling analysis* and which we believe to be a useful statistical test in the study of chaotic or stochastic systems. In the remainder of this section we briefly introduce this method and we show how it may be applied to the analysis of the colored random noises discussed here.

To develop the concept of scaling space we first consider the motion of a system in an N-dimensional phase space. Each component of the motion is given by $X_n = X_n(t_i)$, where n ranges over the number of phase space dimensions N, while i ranges over the number of points M in the time series. The N-component time series $X_n(t_i)$ may either be N independent measurements of the dynamics or the N delayed variables obtained by a time-embedding procedure. We then define time series of the dynamical (amplitude) scales of the $X_n(t_i)$ as

$$s_n\left(t_{(i-1)M+j}\right) = X_n(t_i) - X_n(t_j) \tag{5.1}$$

for $i, j = 1, 2, \ldots, M$, $i \neq j$. We refer to the $s_n(t_i)$ as the *coordinates in (an N-dimensional) scaling space*. The original time series are assumed to have M points, hence the *time series of scales* (5.1) have $M^2 - M$ points. One then constructs a joint probability density function over all the scaling space coordinates, $p(s_1, s_2, \ldots, s_N)$. This density function may be exploited in its own right (see discussion below); we first however discuss its relationship to the classic Grassberger and Procaccia approach. To this end consider an appropriate norm of the vector $s = (s_1, s_2, \ldots, s_N)$, such as the Euclidean norm which is used here

$$r(t_i) = \left\{ s_1(t_i)^2 + s_2(t_i)^2 + \cdots + s_N(t_i)^2 \right\}^{1/2}, \tag{5.2}$$

and suitable definitions for appropriate $N-1$ angle coordinates, say $\theta_1, \theta_2, \ldots, \theta_{N-1}$, which we write symbolically

$$s_n = r f_n(\theta_1, \theta_2, \ldots, \theta_{N-1}), \tag{5.3}$$

Note that the f_n are functions only of the θ_n and not of r or the s_n. Transforming the joint density of scales $p(s_1, s_2, \ldots, s_N)$ by (5.2), (5.3) we find a joint density function in N-dimensional spherical coordinates:

$$p(r, \theta_1, \theta_2, \ldots, \theta_{N-1}) = r^{N-1} p(r f_1, r f_2, \ldots, r f_N). \tag{5.4}$$

Integrating (5.4) over all the angles θ_n gives the one-dimensional density $p(r)$. The integral distribution associated with $p(r)$ is the correlation function

$$C_N(\varepsilon) = \int_0^{\varepsilon} p(r)\, dr. \tag{5.5}$$

Eq. (5.5), for a simple rectangular discretization, is equivalent to the correlation function of Grassberger and Procaccia [16]. The correlation dimension is given by $\nu \approx \log C_N(\varepsilon) / |\log \varepsilon|$ for large N and small ε and is thus easily recovered in the framework of multivariate scaling analysis.

The approach described by (5.1)–(5.5) has the capability of providing a larger amount of information than the simple calculation of the fractal dimension. While the fractal dimension is related to the local, small-scale properties of the system (i.e. the behavior of $p(s)$ for $|s| \approx 0$), the study of the probability distribution $p(s)$ for all s gives information on the *global* properties of the system. Thus multivariate scaling analysis provides a new framework for the determination of some of the statistical and scaling properties of a system over all scales of the motion. In the present application the approach provides graphic evidence of the non-Gaussian behavior of the scales for stochastic systems with power-law spectra.

To this end we consider several cases which illustrates the global scaling behavior of colored random noises. For graphical purposes we consider the two-dimensional densities $p(s_x, s_y)$ and their associated contours. To compute these we consider pairs of phase space coordinates (x, y) which are selected as separate realizations of the stochastic processes $x(t; \alpha)$ and $y(t; \alpha)$. In what follows we have used two sets of random numbers, one for the time series $x(t; \alpha)$, the other for $y(t; \alpha)$. Time series of 32768 points have been computed for both $x(t; \alpha)$ and $y(t; \alpha)$ for the following values of the spectral exponent: $\alpha = 0.0$, 1.0, 1.50, 1.67, 1.75, 2.00, 2.50, 3.00, 5.00 and 8.00. The time series have been normalized to have a standard deviation of $\sqrt{2}$. The results of these simulations are shown in fig. 15. The first case corresponds to $\alpha = 0.00$ (fig. 15(a)), normally referred to as white

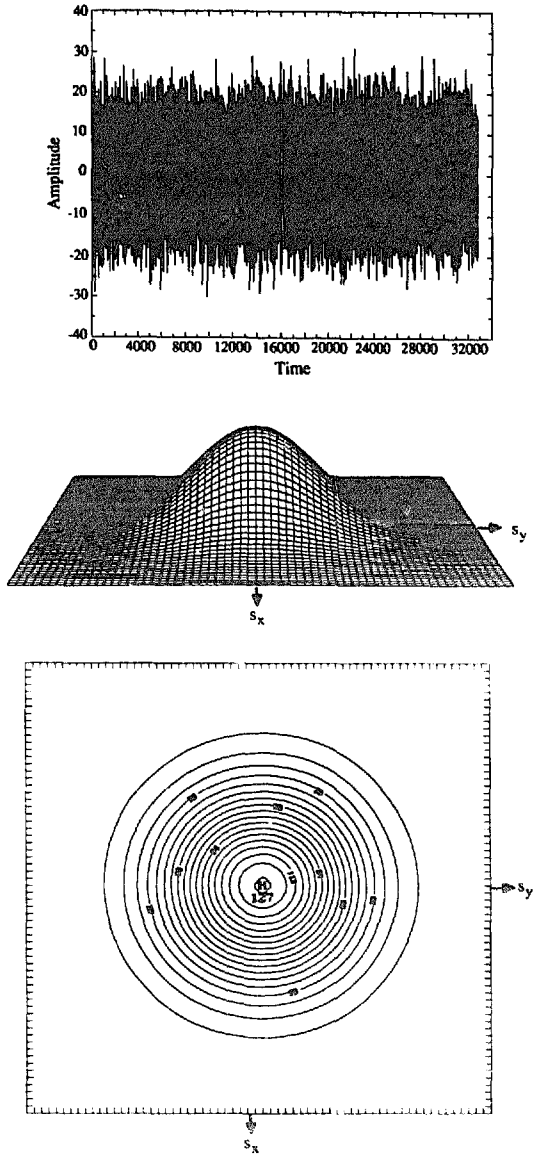

Fig. 15(a).

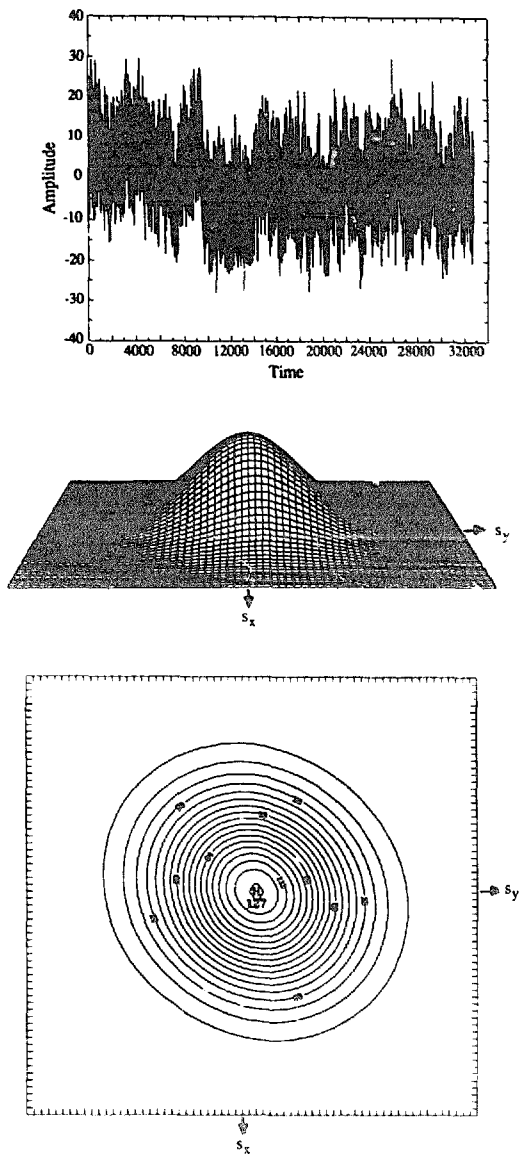

Fig. 15(j).

Fig. 15. Multivariate scaling analysis of colored noise for $\alpha = 0.0$, $D \to \infty$. Shown are the time series $x(t; \alpha)$ (top), the multivariate density $p(s_x, s_y)$ (middle) and contours of $p(s_x, s_y)$ (bottom). (a) $\alpha = 0.0$, $D \to \infty$. (b) $\alpha = 1.0$, $D \to \infty$. (c) $\alpha = 1.5$, $D = 4.00$. (d) $\alpha = 5/3 = 1.66\ldots$, $D = 3.00$. (e) $\alpha = 1.75$, $D = 2.67$. (f) $\alpha = 2.0$, $D = 2.00$. (g) $\alpha = 2.5$, $D = 1.33$. (h) $\alpha = 3.0$, $D = 1.00$. (i) $\alpha = 5.0$, $D = 1.0$. (j) $\alpha = 8.0$, $D = 1.00$.

noise. The time series of $x(t;\alpha)$ is shown in the first panel; we do not graph the time series $y(t;\alpha)$ (another realization of the same process which closely resembles $x(t;\alpha)$) for the sake of brevity. From the time series $x(t;0)$ and $y(t;0)$ we form the scales by (5.2) and then build a two-dimensional histogram of $p(s_x, s_y)$, which we graph on the intervals $-5 \le s_x \le 5$, $-5 \le s_y \le 5$. In the middle panel we show the two-dimensional density function $p(s_x, s_y)$ which is clearly Gaussian in the present case; the contours are perfect circles as shown in the lower panel. The correlation dimension for this case is theoretically infinity. The case for "one over f noise" ($\alpha = 1.00$) is given in fig. 15(b). The time series (top panel), two-dimensional scaling density function (middle panel) and contours (bottom panel) are given. Small deviations from Gaussinity are evident, especially in the contours; the correlation dimension is again infinity (see eq. (4.5)). Fig. 15(c) gives the results for

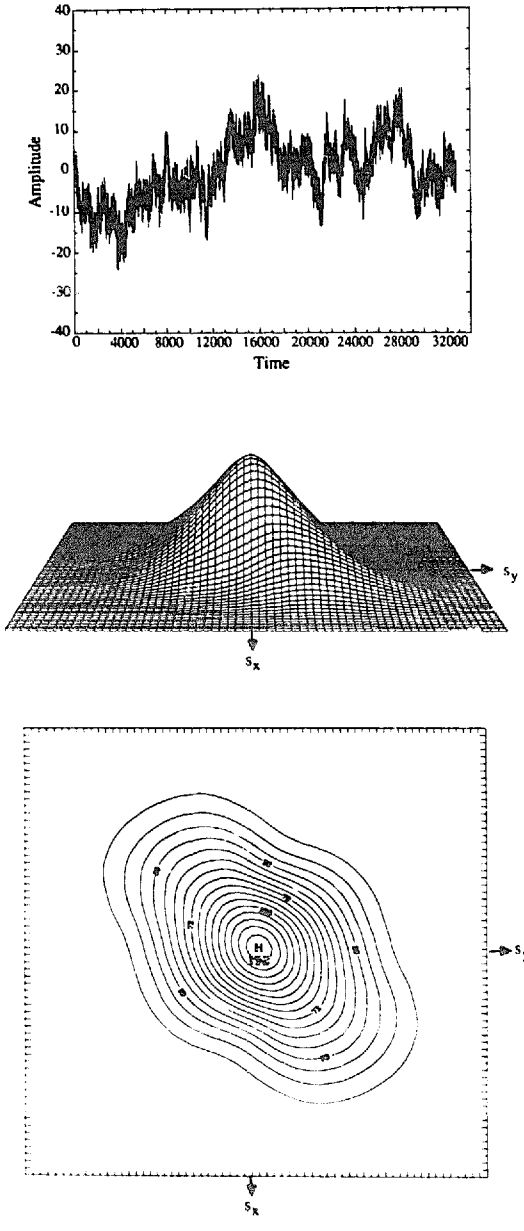

Fig. 15(c).

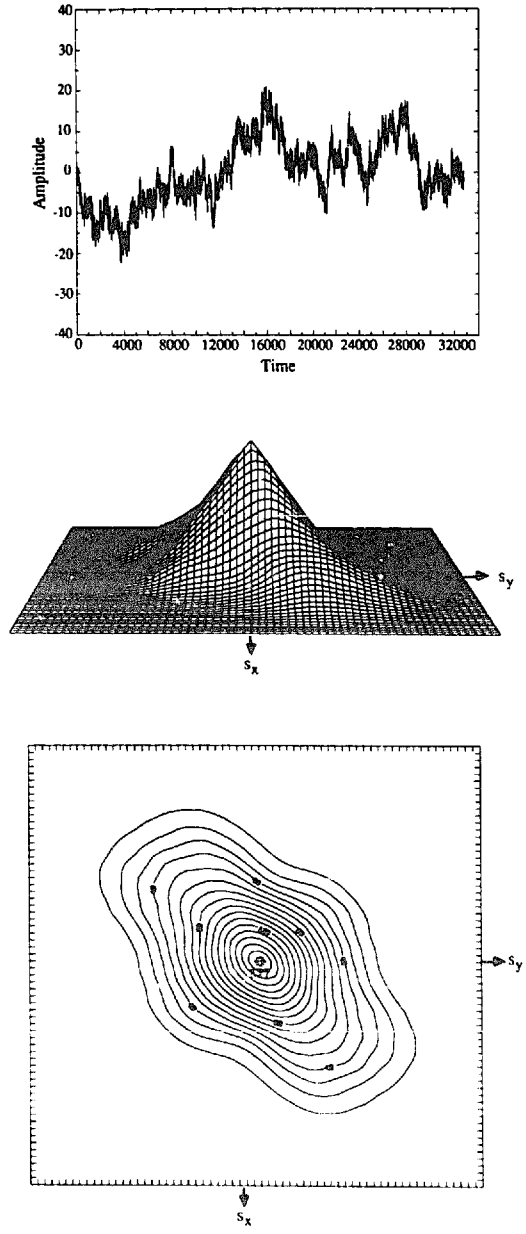

Fig. 15(d).

$\alpha = 1.50$. Note that the scales are distinctly non-Gaussian for this case in which the correlation dimension is given by $D = 4.0$. Note that as we increase α the high-frequency structure of the time series simplifies as the low-frequency motions begin to dominate more and more the power spectrum.

The case $\alpha = 5/3$, relevant for fully-developed, three-dimensional Eulerian turbulence, is given in fig. 15(d). The deviations from Gaussian behavior are somewhat enhanced from the previous case, but may be viewed as only small excursions from Gaussinity. The theoretical correlation dimension is $D = 3.0$. Fig. 15(e) shows the results for $\alpha =$

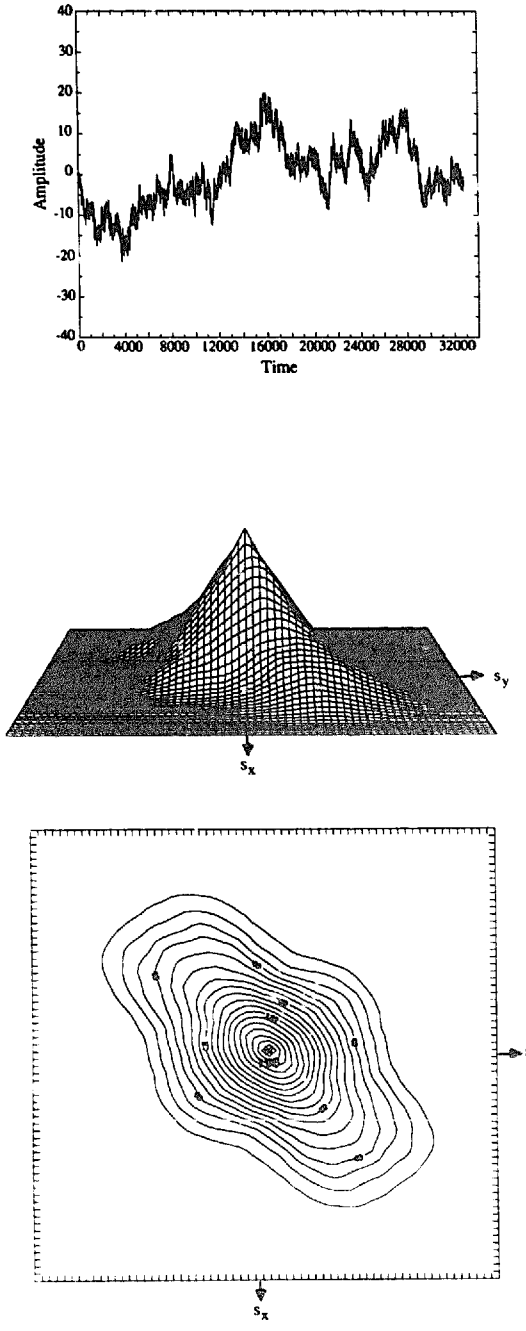

Fig. 15(e).

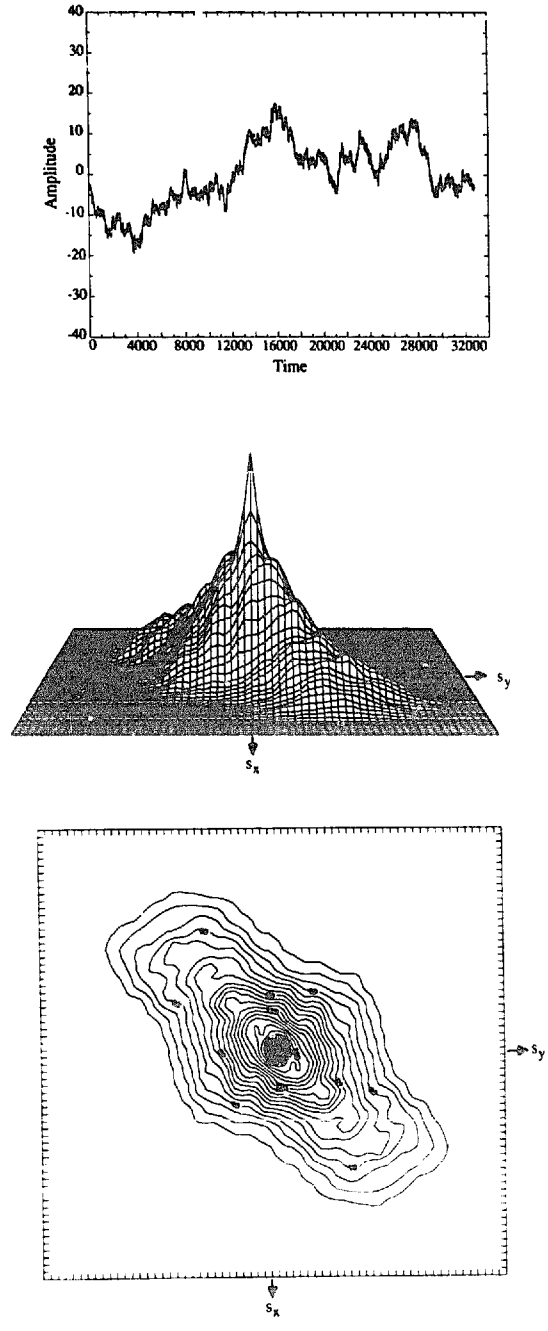

Fig. 15(f).

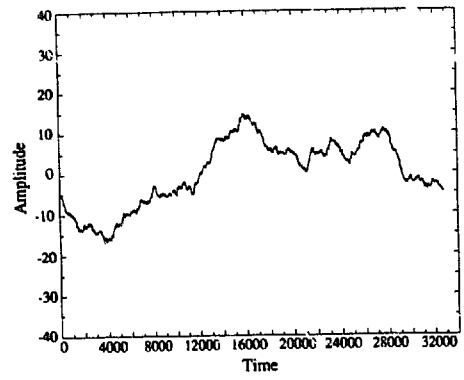

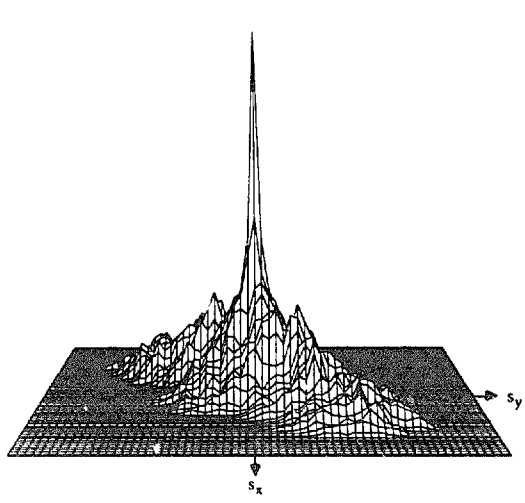

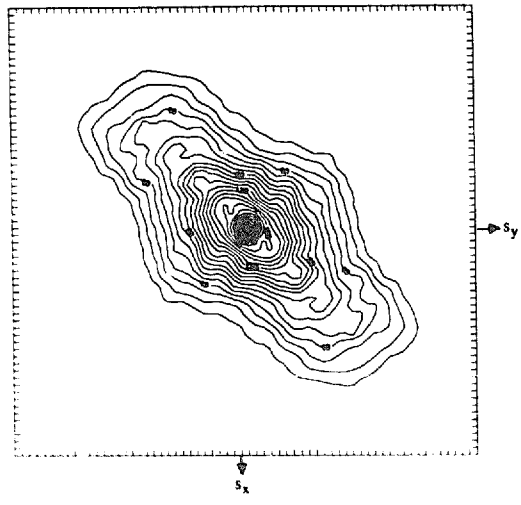

Fig. 15(g).

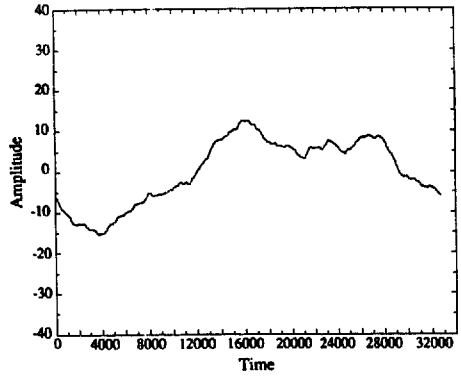

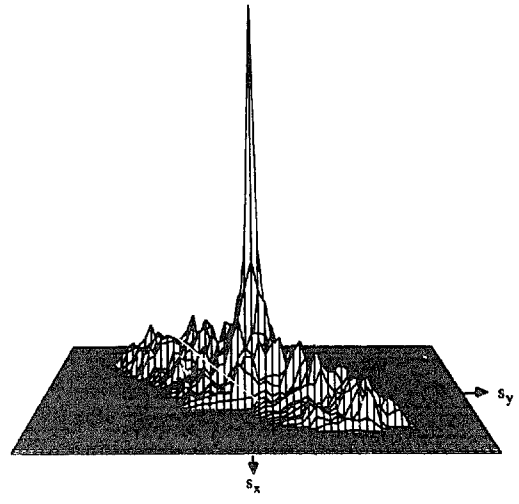

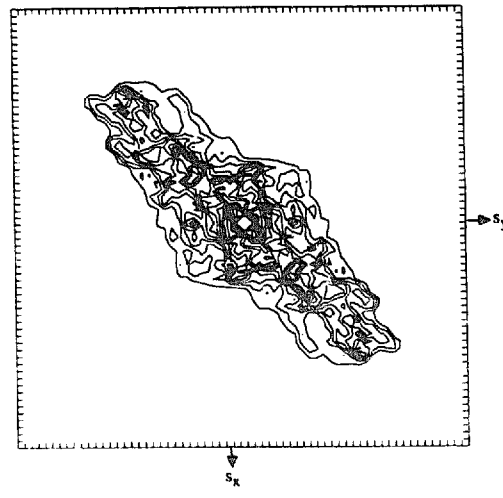

Fig. 15(h).

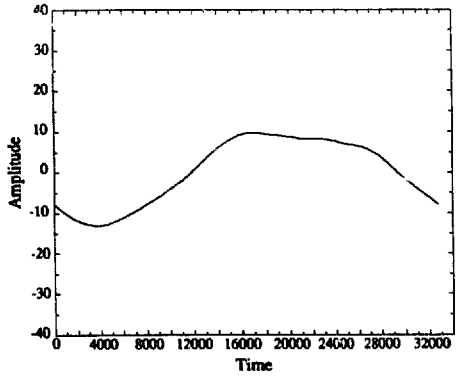

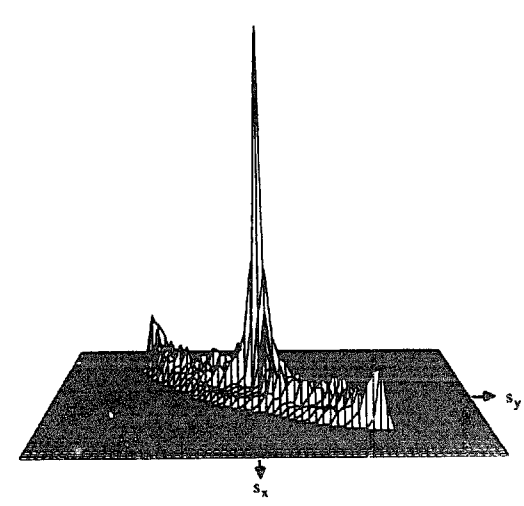

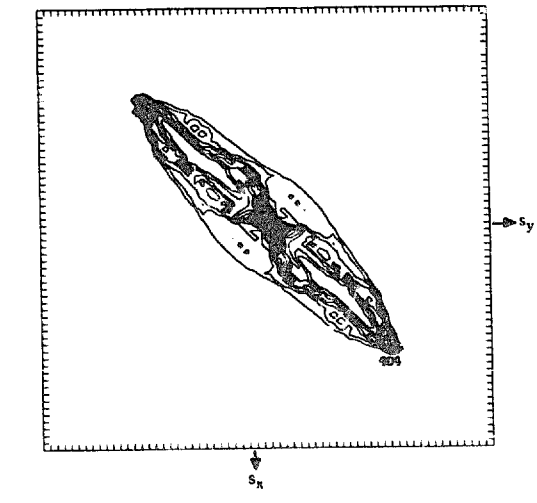

Fig. 15(i).

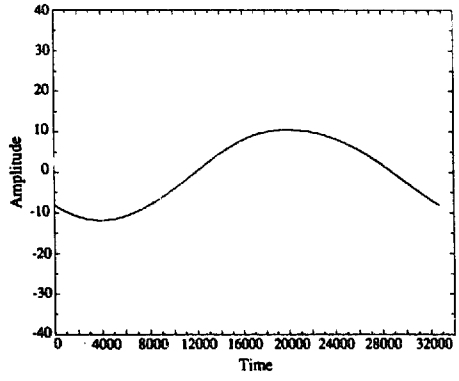

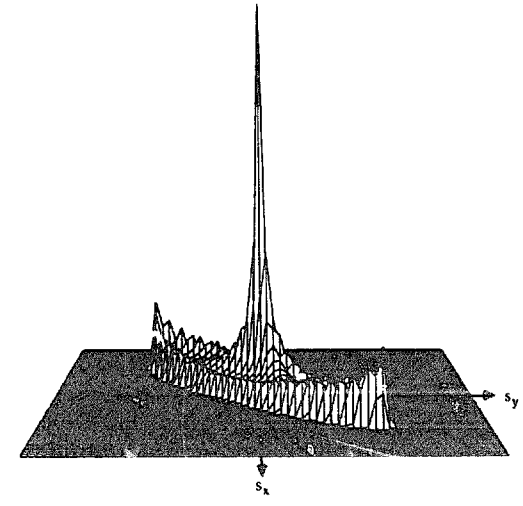

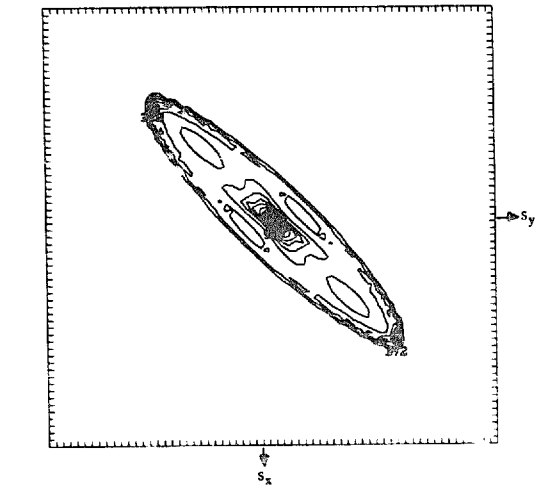

Fig. 15(j).

1.75; note that the scaling density is beginning to show a distinct sharp peak with the associated fractal dimension given by $D = 2.67$. The case $\alpha = 2.00$ (a value often assumed for fully-developed, isotropic, three-dimensional Lagrangian turbulence) is shown in fig. 15(f). A distinct peak is now evident near the origin of the scaling density function. The dimension is given theoretically by $D = 2.00$. The next case is that for which $\alpha = 2.50$ (fig. 15(g)) and was chosen because it has been shown experimentally to be relevant to results of experimental measurements in a geophysical fluid dynamical flow [30]. Here the dimension is $D = 1.33$. The subsequent case ($\alpha = 3.0$) is interesting because it occurs exactly at that value of the spectral exponent for which the correlation dimension is reduced to $D = 1.00$ (fig. 15(h)). The remaining two cases ($\alpha = 5.00$ and 8.00) also have dimension $D = 1.00$ (figs. 15(i) and 15(j)). Note that the time series $x(t; 8.00)$ is almost a sine wave; this occurs because of the steep value of the exponent which results in the first (low-frequency) component dominating the energy in the spectrum.

The results of the multivariate scaling analysis of the Monte Carlo simulations of colored random noise may be interpreted as follows. The fractal nature of the time series arises because of the non-Gaussian convergence of the Fourier series (3.1); this results because the central limit theorem fails for the special case of power-law spectra, and non-Gaussian statistical behavior of the time series $x(t; \alpha)$ and the scales of motion $s_x(t)$ occurs. Generally speaking an increase in the spectral exponent α causes increasing deviations from Gaussian behavior. The multivariate densities $p(s_x, s_y)$ are Gaussian in the case of white noise ($\alpha = 0.0$, fig. 15(a)) and the fractal dimension is infinite. "One over f" noise ($\alpha = 1.0$, fig. 15(b)) is nearly Gaussian and still infinite dimensional. Further increases in α begin to cause increasing non-Gaussian behavior in the two-dimensional density function $p(s_x, s_y)$. One aspect of the non-Gaussinity is that a central peak forms at small scales as α is increased; a sharp peak for $|s| \approx 0$ implies a low value of the fractal dimension. Some interesting physical cases with power-law spectra are those for 3-D turbulence ($\alpha = 1.66\ldots$, $D = 3.0$, fig. 15(d)), internal waves ($\alpha = 2.0$, $D = 2.0$, fig. 15(f)), Lagrangian geophysical fluid dynamical turbulence ($\alpha = 2.5$, $D = 1.33$, fig. 15(g)) and the simple cycle ($\alpha = 8.0$, $D = 1.0$, fig. 15(j)). While it is unclear whether the random phase approximation is appropriate for these and other important physical systems, it seems clear that future studies will reveal how the multivariate scaling approach may be exploited in the analysis of experimental data, also when the phases are not randomly distributed.

6. Summary and discussion

We have studied a class of stochastic processes characterized by power spectra with power-law dependence and random, uniformly distributed Fourier phases. We have shown that *these colored random noises provide a finite and predictable value for the correlation dimension*. The results of this research thus provide a counter-example to the general belief that random signals give a non-saturating value for the correlation dimension. The finite dimensions have subsequently been shown to be generated by the fractal properties of the random signals. These "colored" random noises in fact are self-affine signals which, when used as a parametric representation of an N-dimensional curve, generate a fractal curve whose dimension is completely determined by the power spectral exponent α. Thus for this class of random processes there is a one-to-one correspondence between the power-law dependence of the spectrum and fractal behavior. We note that this one-to-one correspondence is not necessarily observed for all systems with power-law spectra since the randomness of the Fourier phases is the other important ingredient. This furthermore implies that in general the sole observation of power-law spectra does not allow for immediately inferring

the fractal nature of the corresponding signals and the value of the fractal dimension.

In our opinion the results discussed here have implications on experimental studies of deterministic chaos. The methods developed in recent years to compute the fractal dimension of strange attractors are in fact widely used on experimental time series from dissipative systems to determine the possible presence of low-dimensional chaotic dynamics. The usual expectation is that if a finite and small fractal dimension is determined, then the system is thought to be dominated by a low-dimensional strange attractor. Traditionally in fact systems dominated by some kind of stochastic process are thought to provide a non-saturating value of the dimension. *The present analysis shows on the contrary that observing a finite correlation dimension from experimental data does not necessarily imply the presence of deterministic chaos, as there are stochastic processes which give a finite value of the fractal dimension that is clearly not related to any deterministic dynamics.* Care must thus be exercised in concluding that a strange attractor exists from the sole calculation of the fractal dimension from an experimental (or numerical) system whose exact dynamics are not sufficiently understood. In particular finite fractal dimensions from systems with power-law spectra must be interpreted with caution since they may be generated by the fractal (non-deterministic) properties of stochastic processes with this kind of spectra. We mention in addition that also the K_2 entropy (another well-known "test" for chaoticity, see Grassberger and Procaccia [17]) has a finite and predictable value for the class of random processes with power-law spectra considered here [30]. Hence, also this procedure apparently does not allow for distinguishing between deterministic chaos and random noise. The convergence of the K_2 entropy is essentially related to the convergence of the correlation dimension itself and will be discussed in a forthcoming paper. Generally speaking other tests must be applied to the data in order to determine the presence of low-dimensional chaos. Among these, for example, are a computation of the spectrum of Lyapunov exponents, or, possibly, the recently developed methods based on singular value decomposition of the system dynamics (see Broomhead and King [6], King et al. [22]) or on the study of the unstable periodic orbits of the system, see Procaccia [34]. The application of these methods to field data is however still unknown.

In the spirit of developing new time series analysis methods applicable to stochastic or deterministic systems we have discussed a new technique which we call *multivariate scaling analysis*. This method is based on the probability distribution $p(s)$ of the amplitude scales s of the system and has the capability of providing statistical information on both local and global properties of the system. The correlation dimension in particular (which is a local property) may be easily determined from the behavior of $p(s)$ in the vicinity of $|s| = 0$. New information on the global properties of the system may also be obtained from the large-scale behavior of $p(s)$. Although this method is probably not *the* solution to the problem of distinguishing between deterministic chaos and stochastic randomness, we believe that its careful usage may be useful for gaining additional information on the nature of experimentally measured or numerically generated signals. The approach thus provides a new tool in the arsenal of methods available to the experimenter for the investigation of chaotic effects in measured time series.

Acknowledgements

We acknowledge Professor C. Castagnoli, Director of the Istituto di Cosmo-Geofisica del Consiglio Nazionale delle Ricerche, for continuing support and valuable encouragement. This research has received funding from the Consiglio Nazionale delle Ricerche and from the Ministero della Pubblica Istruzione. During part of this research one of us (A.P.) was supported by a fellowship of the Dottorato di Ricerca in Fisica at the University of Torino.

Appendix

Discussion of the role of time-embedding procedures

As anticipated in section 3 an interesting issue is whether the use of a time-embedding procedure (as opposed to the use of independent realizations which was considered here) could modify the results of the analysis. There is often the hope that a simple time-embedding procedure might miraculously disentangle an unknown dynamical motion. Thus a brief discussion of embedding is appropriate here.

We first note that a choice of an appropriate time delay for the embedding may be difficult since the random noises considered here have a long "memory" and their autocorrelation functions tend to zero quite slowly. In order to satisfy the requirements of mutual independence of the various time-delayed values in the embedding we must thus select a sufficiently large value for the delay. This can be achieved either by choosing the time delay larger than an appropriately defined "decorrelation time" (see for example Panchev [33]) or, better, by using the procedure based on the calculation of the amount of mutual information recently proposed by Fraser and Swinney [13]. The main result is that, if the time delay is sufficiently large, then the calculated values of the correlation dimension are independent of the value of the delay and coincide with the results obtained using independent realizations.

For time delays smaller than the appropriate decorrelation time the estimates of the dimension depend, even if slowly, on the time delay itself and are in general larger than the correct values predicted by the theoretical relation (4.5) or by its generalization to truncated power spectra. This behavior is spuriously generated by the correlations among the different "pseudo-phase space variables" introduced by the embedding. It is important to stress that also in this case, when it is possible to define a scaling range, the saturation of the correlation dimension is always observed, i.e. *one always obtains a finite value for the correlation dimension of a random signal* with a power-law spectrum and random phases.

References

[1] P. Atten, J.G. Caputo, B. Malraison and Y. Gagne, Determination of attractor dimension of various flows, J. Mech. Theor. Appl., special issue (1984) 133–156.
[2] R. Badii and A. Politi, Hausdorff dimension and uniformity factor of strange attractors, Phys. Rev. Lett. 52 (1984) 1661–1664.
[3] G.K. Batchelor, Small-scale variation of convected quantities like temperature in turbulent fluid. Part 1. General discussion and the case of small conductivity, J. Fluid Mech. 5 (1959) 113–133.
[4] P. Bergé, Study of phase space diagrams through experimental Poincaré sections in prechaotic and chaotic regimes, Physica Scripta T 1 (1982) 71.
[5] A. Brandstater, J. Swift, H.L. Swinney, A. Wolf, J.D. Farmer, E. Jen and P.J. Crutchfield, Low-dimensional chaos in a hydrodynamic system, Phys. Rev. Lett. 51 (1983) 1442–1445.
[6] D.S. Broomhead and G.P. King, Extracting qualitative dynamics from experimental data, Physica D 20 (1986) 217–236.
[7] S. Ciliberto and J.P. Gollub, Pattern competition leads to chaos, Phys. Rev. Lett. 52 (1984) 922–925.
[8] S. Ciliberto and J.P. Gollub, Chaotic mode competition in parametrically forced surface waves, J. Fluid Mech. 158 (1985) 381.
[9] J.P. Eckmann and D. Ruelle, Ergodic theory of chaos and strange attractors, Rev. Mod. Phys. 57 (1985) 617–656.
[10] J.D. Farmer, E. Ott and J.A. Yorke, The dimension of chaotic attractors, Physica D 7 (1983) 153–80.
[11] A. Fote, J. McDonough and R. Egler, Chaos theory and $1/f$ noise in HgCdTe photodiodes, Nucl. Phys. B (proc. suppl.) 2 (1987) 597.
[12] K. Fraedrich, Estimating the dimensions of weather and climate attractors, J. Atmos. Sciences 43 (1986) 419–432.
[13] A.M. Fraser and H.L. Swinney, Independent coordinates for strange attractors from mutual information, Phys. Rev. A 33 (1986) 1134–1140.
[14] H. Froehling, J.P. Crutchfield, J.D. Farmer, N.H. Packard and R. Shaw, On determining the dimension of chaotic flows, Physica D 3 (1981) 605–617.
[15] C.J.R. Garrett and W.H. Munk, Internal waves in the ocean, Ann. Rev. Fluid Mech. 11 (1979) 339–369.
[16] P. Grassberger and I. Procaccia, Measuring the strangeness of strange attractors, Physica D 9 (1983) 189–208.
[17] P. Grassberger and I. Procaccia, Estimation of the Kolmogorov entropy from a chaotic signal, Phys. Rev. A 28 (1983) 2591–2593.
[18] H.S. Greenside, A. Wolf, J. Swift and T. Pignataro, Impracticability of box counting algorithms for calculating

the dimension of strange attractors, Phys. Rev. A 25 (1982) 3453–3456.

[19] J. Guckheneimer and G. Buzyna, Dimension measurements for geostrophic turbulence, Phys. Rev. Lett. 51 (1983) 1438–1441.

[20] A. Hense, On the possible existence of a strange attractor for the southern oscillation, Beitr. Phys. Atmosph. 60 (1987) 34–47.

[21] C. Keppenne and C. Nicolis, Toward a quantitative view of predictability of weather patterns, Ann. Geophys., special issue "EGS General Assembly" (1988) 207.

[22] G.P. King, R. Jones and D.S. Broomhead, Phase portraits from a time series: a singular system approach, Nucl. Phys. B (proc. suppl.) 2 (1987) 379–390.

[23] D.C. Leslie, Developments in the Theory of Turbulence (Clarendon, Oxford, 1973).

[24] B. Malraison, P. Atten, P. Berge and M. Dubuois, Dimension of strange attractors: an experimental determination for the chaotic regime of two convective systems, J. Phys. Letters 44 (1983) L897–L902.

[25] B.B. Mandelbrot, Fractals: Form, Chance and Dimension (Freeman, San Francisco, 1977).

[26] B.B. Mandelbrot, The Fractal Geometry of Nature (Freeman, San Francisco, 1982).

[27] R. Mané, On the dimension of the compact invariant sets of certain nonlinear maps, in: Lecture Notes in Mathematics 898, D.A. Rand and L.S. Young, eds. (Springer, Berlin, 1981), pp. 230–242.

[28] C. Nicolis and G. Nicolis, Is there a climatic attractor?, Nature 311 (1984) 529–532.

[29] A.R. Osborne, The simulation and measurement of random ocean wave statistics, in: Topics in Ocean Physics, Proc. Int. School of Physics "E. Fermi", Course LXXX, A.R. Osborne and P. Malanotte Rizzoli, eds. (North-Holland, Amsterdam, 1982), pp. 515–550.

[30] A.R. Osborne, A.D. Kirwan, A. Provenzale and L. Bergamasco, A search for chaotic behavior in large and mesoscale motions in the Pacific Ocean, Physica D 23 (1986) 75–83.

[31] S.A. Orszag, Lectures on the statistical theory of turbulence, in: Fluid Dynamics, Proc. Les Houches, R. Balian and J.-L. Peube, eds. (Gordon and Breach, London, 1977), pp. 235–374.

[32] N.H. Packard, J.P. Crutchfield, J.D. Farmer and R.S. Shaw, Geometry from a time series, Phys. Rev. Lett. 45 (1980) 712–716.

[33] S. Panchev, Random Functions and Turbulence (Pergamon, Oxford, 1971).

[34] I. Procaccia, Exploring deterministic chaos via unsatable periodic orbits, Nucl. Phys. B (proc. suppl.) 2 (1987) 527–538.

[35] G. Radnoti, Characterizing the weather attractor, Ann. Geophys., special issue "EGS General Assembly" (1988) 210.

[36] S.O. Rice, Mathematical analysis of random noise, in: Noise and Stochastic Processes, N. Wax, ed. (Dover, New York, 1954), pp. 133–246.

[37] R. Salmon, Geostrophic turbulence, in: Topics in Ocean Physis, Proc. Int. School of Physics "E. Fermi", Course LXXX, A.R. Osborne and P. Malanotte Rizzoli, eds. (North-Holland, Amsterdam, 1982), pp. 30–78.

[38] H.L. Swinney and J.P. Gollub, Characterization of hydrodynamic strange attractors, Physica D 18 (1986) 448–454.

[39] F. Takens, Detecting strange attractors in turbulence, in: Lecture Notes in Mathematics 898, D.A. Rand and L.S. Young, eds. (Springer, Berlin, 1981), pp. 366–381.

[40] A.A. Tsonis, On the dimension of the weather attractor, Ann. Geophys., special issue "EGS General Assembly" (1988) 208.

[41] A.M. Yaglom, An introduction to the theory of stationary random functions, Uspehy Math. Sci. 7 (1952) (Rev. English ed.: Prentice-Hall, Englewood Cliffs, N.J., 1962).

[42] L.S. Young, Dimension, entropy, and Lyapunov exponents, Ergodic Theory and Dynamical Systems 2 (1982) 109.

[43] A. Wolf, J.B. Swift, H.L. Swinney and J.A. Vastano, Determining Lyapunov exponents from a time series, Physica D 16 (1985) 285–317.